IPEM
Institute of Physics and
Engineering in Medicine

PAPER

Intra-breath changes in respiratory mechanics assessed from multi-frequency oscillometry measurements

View the article online for updates and enhancements.

Physiological Measurement

PAPER

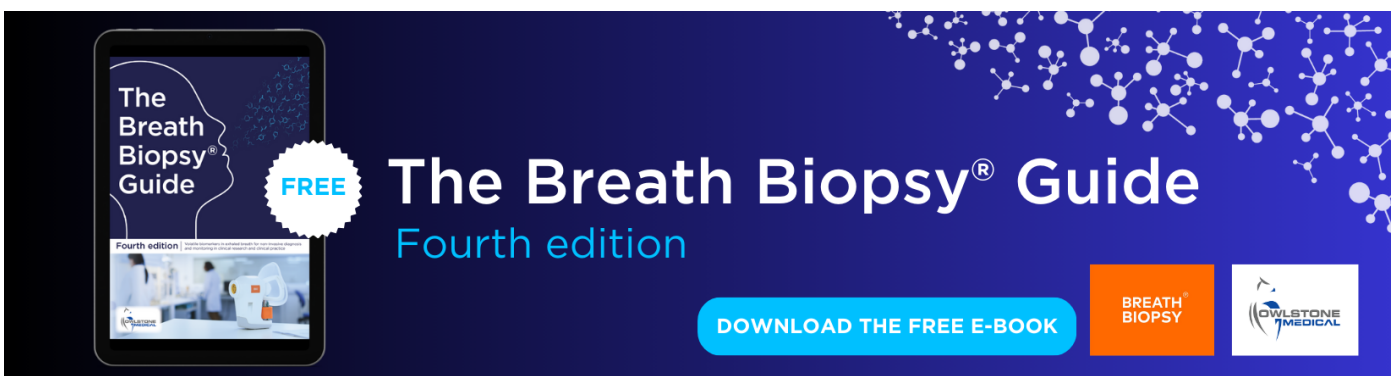# Intra-breath changes in respiratory mechanics assessed from multi-frequency oscillometry measurements

Gergely Makan[1] , Ronald J Dandurand[2,3] , Zoltán Gingl[1] and Zoltán Hantos[1,4]

[1] Department of Technical Informatics, University of Szeged, Szeged, Hungary
[2] Lakeshore General Hospital, Pointe-Claire, QC, Canada
[3] Oscillometry Unit of the Centre for Innovative Medicine, and the Meakins-Christie Laboratories, McGill University Health Centre and Research Institute, and McGill University, Montreal, QC, Canada
[4] Department of Anaesthesiology and Intensive Therapy, Semmelweis University, Budapest, Hungary

E-mail: hantos.zoltan@med.u-szeged.hu

Abstract

Objective. Recent studies in respiratory system impedance (Zrs) with single-frequency oscillometry have demonstrated the utility of novel intra-breath measures of Zrs in the detection of pathological alterations in respiratory mechanics. In the present work, we addressed the feasibility of extracting intra-breath information from Zrs data sets obtained with conventional oscillometry. *Approach.* Multi-frequency recordings obtained in a pulmonology practice were re-analysed to track the 11 Hz component of Zrs during normal breathing and compare the intra-breath measures to that obtained with a single 10 Hz signal in the same subjects. A nonlinear model was employed to simulate changes in Zrs in the breathing cycle. The values of resistance (R) and reactance (X) at end expiration and end inspiration and their corresponding differences (ΔR and ΔX) were compared. *Main results.* All intra-breath measures exhibited similar mean values at 10 and 11 Hz in each subject; however, the variabilities were higher at 11 Hz, especially for ΔR and ΔX. The poorer quality of the 11 Hz data was primarily caused by the overlapping of modulation side lobes of adjacent oscillation frequencies. This cross-talk was enhanced by double breathing frequency components due to flow nonlinearities. *Significance.* Retrospective intra-breath assessment of large or special data bases of conventional oscillometry can be performed to better characterise respiratory mechanics in different populations and disease groups. The results also have implications in the optimum design of multiple-frequency oscillometry (avoidance of densely spaced frequencies) and the use of filtering procedures that preserve the intra-breath modulation information.

1. Introduction

Respiratory oscillometry (also termed commonly as the forced oscillation technique,) is a sophisticated and versatile method with a widespread application in respiratory physiology (Bates *et al* 2011, Kaczka and Dellaca, 2011). Oscillometry has become an emerging lung function measurement method in clinical practice (Goldman, 2001, Kalchiem-Dekel and Hines, 2018, Oostveen *et al* 2013, Oostveen *et al* 2003), which was facilitated by the technological advancements allowing fast and easy measurements of Zrs simultaneously at different frequencies. For the sake of the convenient use of the arsenal of linear systems analysis, it was tacitly supposed that respiratory mechanics can be described as a linear time-invariant system (Goldman, 2001, Làndsér *et al* 1976, Michaelson *et al* 1975, Oostveen *et al* 2003), despite early evidence that Zrs changes between different volume levels of natural breathing (Michaelson *et al* 1975, Nagels *et al* 1980) and the demonstration of marked fluctuations in Rrs with flow (Davidson *et al* 1986a, Horowitz *et al* 1983, Peslin *et al* 1971, Peslin *et al* 1992). While the intra-breath variations in Zrs have been shown to introduce a bias in the frequency dependence of Rrs and Xrs (Alamdari *et al* 2019a) and raise concerns about the interpretation and utility of Zrs averaged for

whole breathing cycles, recent studies with single-frequency oscillometry and improved temporal resolution have identified new, clinically meaningful intra-breath measures (Dellacà *et al* 2004, Czövek *et al* 2016, Lorx *et al* 2017, Gray *et al* 2018, Chiabai *et al* 2021, Hantos, 2021). In light of the rapidly growing data bases of conventional multi-frequency oscillometry covering different respiratory diseases, age groups, both sexes and ethnicities, investigation of the possibilities of intra-breath re-analysis on these data may be of clinical importance.

The present study was undertaken to explore the possibilities and limits of intra-breath tracking of Zrs by comparing the measurements obtained with a conventional multi-frequency signal and a single-frequency research modality of a commercial device in a convenience sample of pulmonology patients including both male and female subjects. Additionally, a simple nonlinear model of respiratory mechanics driven by sinusoidal or recorded breathing signals was employed to assess the intra-breath performances of the two signal types and the role of the signal filtering techniques.

2. Methods

2.1. Subjects

Test oscillometry recordings were collected in adult subjects of both sexes in a community respiratory practice clinic (Clinique pneumo Dandurand, Pointe-Claire, QC, Canada) involving patients with a diagnosis of COPD ($n = 16$), interstitial lung disease (ILD, $n = 10$) and asthma ($n = 15$) in 2018, and healthy adult subjects recruited from laboratory staff and attendees of a 2017 World COPD Day open house who underwent screening measurements ($n = 14$). All subjects were white with the exception of one black asthma subject. The 4 subject groups were similar in anthropometry and overall sex distributions did not differ (table S1 in the online supplement.), except that the healthy subjects were younger (median age: 46 year). In this retrospective study, no sample size calculation was employed; the subjects (23 males and 32 females; median age: 70 year) were selected solely to represent a variety of Zrs ranges and breathing patterns. The selection was unrelated to diagnostic comparisons between subgroups of the studied population including sex distribution, given that each subject served as his or her own control; the only inclusion criterion was a minimum number of artefact-free breathing cycles (see below).

2.2. Measurements

The oscillometry measurements analyzed in this study were obtained with a commercial device (tremoflo C-100, Thorasys Medical Inc., Montreal, QC, Canada).This equipment uses a pseudorandom composite signal that includes all relative prime number frequencies in the 5-37 Hz range except the 7 Hz. In each subject,a minimum of three 16 s recordings without breathing artifacts and of sufficient reproducibility were collected. The device was then switched into the single-frequency research modality to measure Zrs at 10 Hz for a 30 s period. The 10 Hz measurement was repeated, if necessary, 1 or 2 times until a sufficient number of breathing cycles (≥ 5) were collected in each subject.

2.3. Analysis

The recordings were exported into a custom-made oscillometry software for intra-breath analysis on the time samples ($256\,\mathrm{s}^{-1}$) of flow (V'), volume (V) and pressure (P). Fast Fourier transformation was employed to calculate Rrs and Xrs at 10 Hz (R10 and X10, respectively), for all successive 0.1 s time windows, following band-pass filtering of V' and P between 8 and 12 Hz. In the case of the 5–37 Hz signal, the corresponding 11 Hz values (R11 and X11) were computed with filter corner frequencies of 9.5 and 12.5 Hz, for successive 1/11 s time windows. In most cases, two-window moving averages of the Rrs and Xrs samples were necessary to reduce the effects of noise.

Linear interpolation was used to establish zero-crossings of V', i.e. the time of end expiration (eE) and end inspiration (eI), and the corresponding Rrs and Xrs values. Since the latter represent zero-flow values, they approximate resistance and reactance of the respiratory system without the influence of flow nonlinearities dominating in the upper airways. The differences in Rrs and Xrs between eE and eI (ΔRrs and ΔXrs, respectively) and their values normalised by tidal volume (V_T), as well as the area of the Xrs versus V loop (AXV) were also selected as primary intra-breath variables.

2.4. Simulations

A simple model of respiratory impedance was formulated to illustrate the contribution of V'- and V-dependent nonlinearities to the spectral shape of the P–V' relationship.

$$P(t) = V'(t)\left[R_0 + k_1|V'(t)| - k_2\,R_0\frac{V(t)}{V_0 + V(t)} \right]$$
$$+ [V_0 + V(t)][E_0 + k_3\,V(t)],$$

where R_0 and E_0 are the end-expiratory resistance and elastance, respectively, k_1 is the coefficient of the V' dependence of resistance (Rohrer 1915), k_2 is the coefficient of an inverse dependence of resistance on V and k_3 determines the change in elastance as a function of $V(t)$ in the tidal volume range. V_0 is the end-expiratory volume. This formulation is similar to that proposed earlier (Peslin *et al* 1971), apart from the inclusion of elastic nonlinearity (k_3) and the omission of inertial properties.

The input signal V' is the sum of the tidal (spontaneous) breathing $V'_{br}(t)$ and the superimposed small-amplitude oscillatory $V'_{osc}(t)$ components

$$V'(t) = V'_{br}(t) + V'_{osc}(t),$$

where V'_{br} was either sinusoidal or selected from typical spirograms recorded in study subjects and low-pass filtered at 4 Hz. The oscillatory component is

$$V'_{osc}(t) = \sum_n (A_n\cos{(n2\pi f_0 t + \varphi_n)}),$$

where n denotes the multiples of the fundamental frequency $f_0 = 1$ Hz, A_n and φ_n are the amplitude and phase angle, respectively, of the frequency component nf_0. For the single-frequency oscillations $n = 10$ was taken, while for the composite signal the relative primes $n = 5, 11, 13, 17, 19, 23, 29, 31, 37$ were selected, with decreasing amplitudes $A_n \sim 1/f$, in accordance with the tremoflo C-100 signal specification. In the latter case, the phase angles relative to φ_0 were optimised to attain the minimum peak-to-peak size of the composite signal (Daroczy and Hantos, 1990).

The model parameters were set to simulate changes in impedance observed typically in healthy subjects and in patients with lung disease. The simulations focused on the effects of flow nonlinearities and the V'_{br} patterns, and they were not intended to be comprehensive. Three input V'_{osc} signals were used: (a) the 10 Hz sinusoid, (b) the composite 5–37 Hz signal and (c) the 5–37 Hz signal without the 13 Hz component to assess the influence of the latter on the estimation of the 11 Hz quantities. The simulated intra-breath Zrs data were computed from the auto- and cross-correlation spectra of the P and V' signals, as in the case of the recorded signals exported by the tremoflo C-100 measurements (see above).

2.5. Statistics
SigmaPlot v14 (Systat Software, Inc., San Jose, CA, USA) statistical package was employed. Mann–Whitney signed rank test was used in pairwise comparisons between 11 and 10 Hz measures of the spirogram and intra-breath oscillometry data, and to check the effect of sex on basic Zrs measures. Differences were considered significant at values of $P < 0.05$. Linear regression and Bland–Altman analysis (Bland and Altman, 1986) were employed to assess the agreement between the two sets of intra-breath measures.
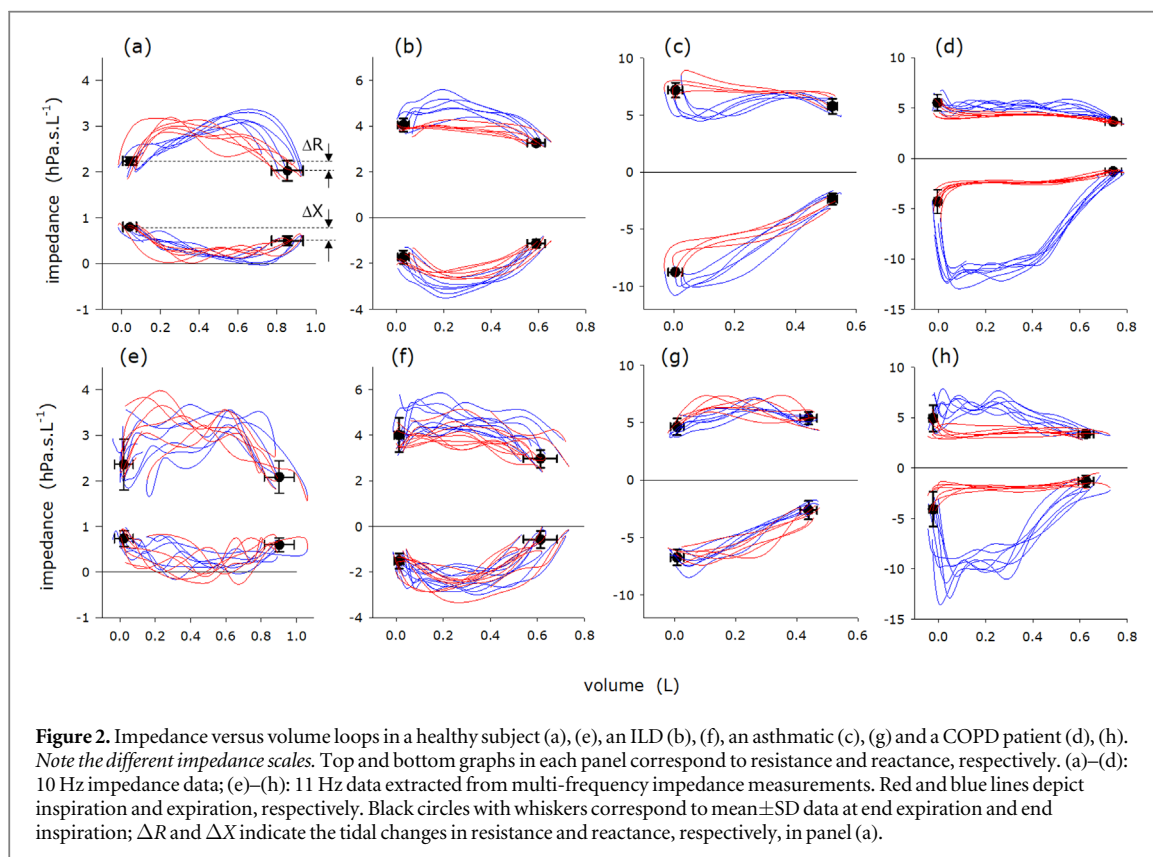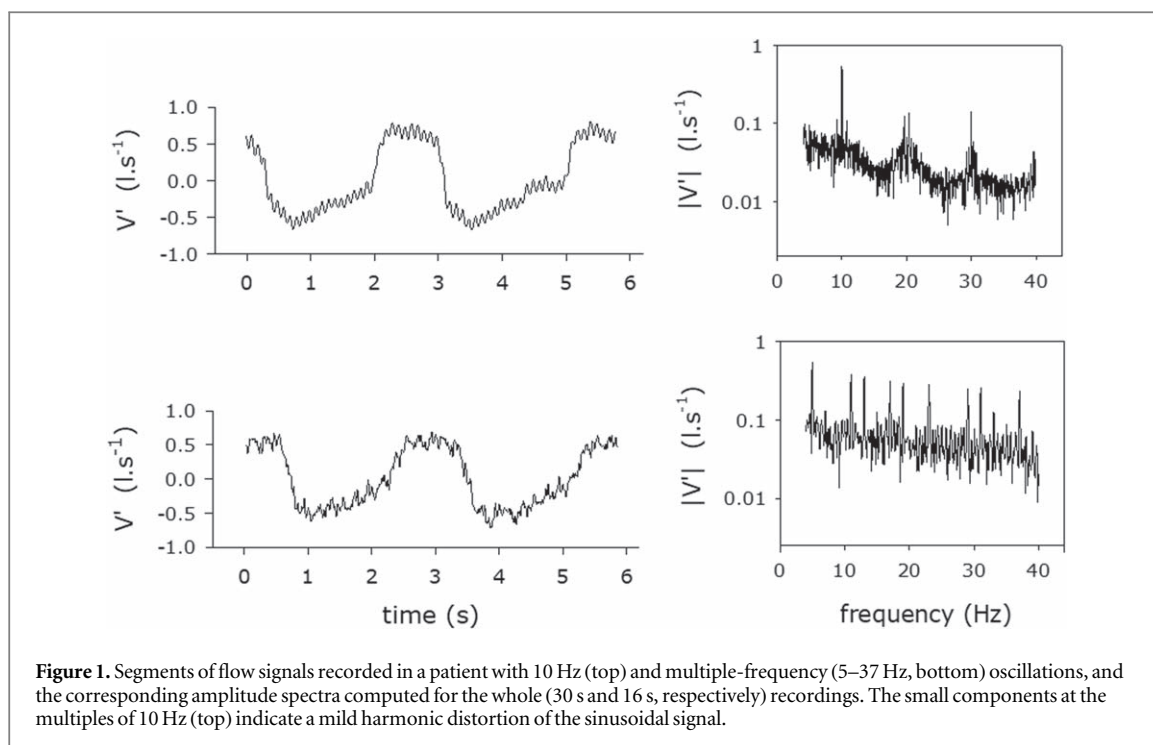
3. Results

3.1. Signal spectra
Figure 1 illustrates the time course and spectral content of the multi- and single-frequency recordings of V' obtained in the same subject. As a consequence of the factory settings of the composite and 10 Hz signals, the amplitude of the latter equalled that of the 5 Hz component of the composite signal where the amplitude of the higher-frequency components decreased inversely with frequency. This means that the 11 Hz component had a roughly half amplitude compared with that of the 10 Hz oscillations.

3.2. Intra-breath changes in Zrs
In figure 2, intra-breath changes in Zrs are illustrated via Rrs versus V and Xrs versus V loops showing different patterns between subjects. Rrs was consistently lower at eI than at eE ($\Delta R > 0$), whereas the tidal change in Xrs was opposite in healthy subjects and patients with lung disease. Massive differences in Xrs between inspiration and expiration (figures 2(d) and (h)) and large AXV loop areas were a typical feature in COPD. All these patterns were similar in the 10–11 Hz recordings from the same subject, although the loops of the latter exhibited less reproducibility, more noise and larger variability in the end-tidal points.

Overall, the intra-breath fluctuations were significant in both Rrs and Xrs. The tidal changes ΔR and ΔX at 10 Hz, expressed as percent changes relative to the end-expiratory Zrs magnitude (Z_{eE}), were 23% (range: -5%–59%) and -18% (-197%–16%), respectively. The peak-to-peak changes in Rrs (R_{pp}) and Xrs (X_{pp}), related to the average of the zero-V' values of Zrs, i.e. $Z_0 = (Z_{eE} + Z_{eI})/2$, amounted to 71% (18%–144%) and 63% (17%–248%), respectively.

Figure 1. Segments of flow signals recorded in a patient with 10 Hz (top) and multiple-frequency (5–37 Hz, bottom) oscillations, and the corresponding amplitude spectra computed for the whole (30 s and 16 s, respectively) recordings. The small components at the multiples of 10 Hz (top) indicate a mild harmonic distortion of the sinusoidal signal.

Figure 2. Impedance versus volume loops in a healthy subject (a), (e), an ILD (b), (f), an asthmatic (c), (g) and a COPD patient (d), (h). *Note the different impedance scales.* Top and bottom graphs in each panel correspond to resistance and reactance, respectively. (a)–(d): 10 Hz impedance data; (e)–(h): 11 Hz data extracted from multi-frequency impedance measurements. Red and blue lines depict inspiration and expiration, respectively. Black circles with whiskers correspond to mean±SD data at end expiration and end inspiration; ΔR and ΔX indicate the tidal changes in resistance and reactance, respectively, in panel (a).

3.3. Comparison of intra-breath measures at 10 and 11 Hz

The end-expiratory and end-inspiratory Rrs values correlated closely (figures 3(a) and (b)), while their differences (ΔR) exhibited more scatter (figure 3(c)). The strong relationships between the X11 and X10 measures (figure 4) are similar to that for R11 and R10; the small systematic differences are consistent with the positive frequency dependence of Xrs (i.e. X10 < X11), expected from both healthy and obstructive subjects. Of note, the X_{eI} values fell into a much narrower range compared with the X_{eE} values (see figures 4(a) and (b)). The

Figure 3. Comparison of 10 and 11 Hz estimates of resistance (R10 and R11, respectively) at end expiration (a) and end inspiration (b), their differences (ΔR, (c)) and the mean values for whole breathing cycles (d). Solid line: line of identity; dashed line: regression line; r^2: correlation coefficient.
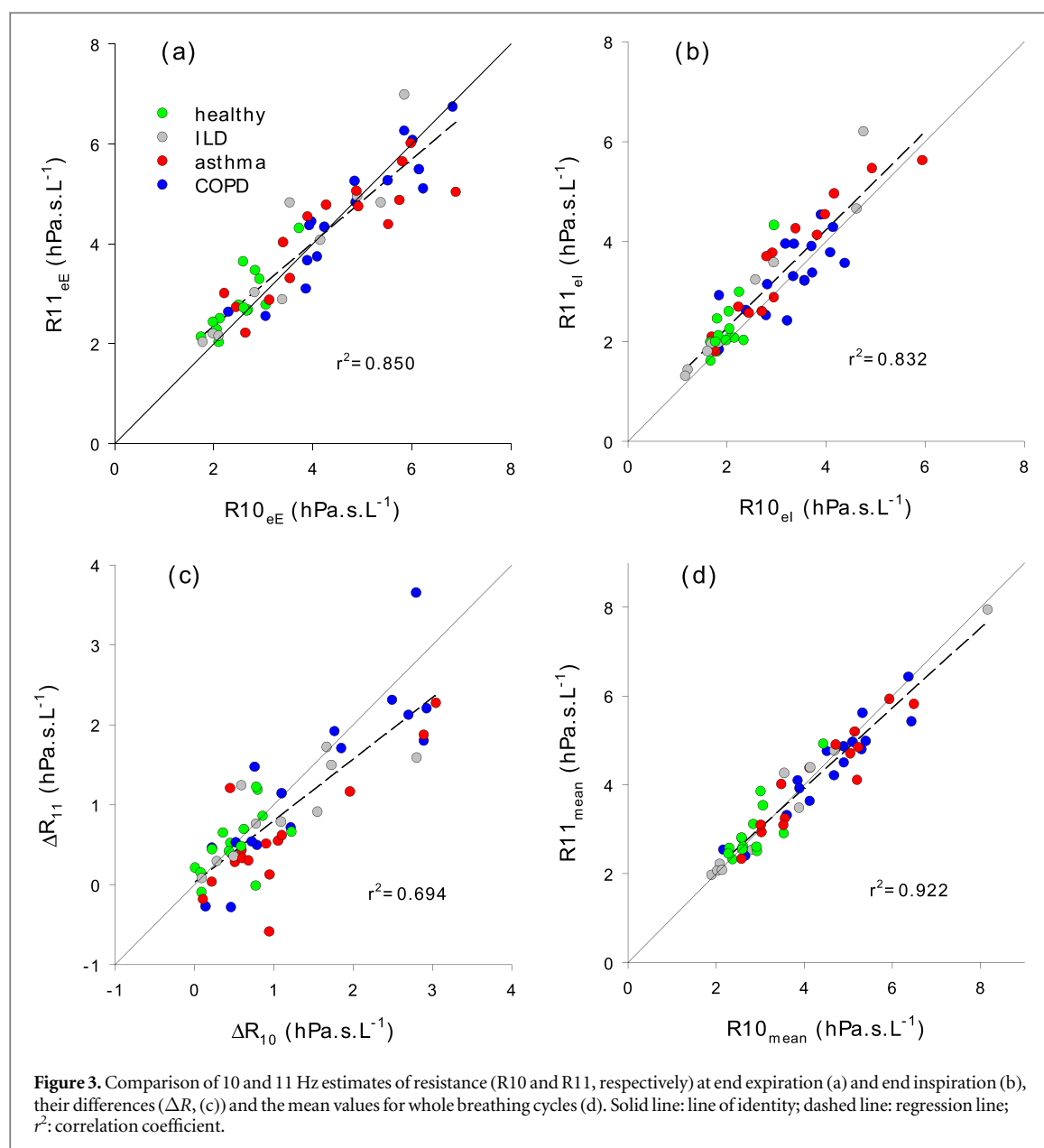
relationship between loop areas AXV11 and AXV10 (figure 4(e)) is similar to that of the other Xrs measures and highlights the dominance of COPD patients at the high AXV values.

Pooled data from the 55 subjects of the study did not show statistically significant differences between the 10 and 11 Hz values (table 1), except that the number of breaths collected from the multi-frequency recordings was slightly higher than that from the 10 Hz measurements in the same subjects (medians: 9 versus 6, $P = 0.02$). However, the within-subject variability of the 11 Hz measures was significantly higher than that of the 10 Hz values in all intra-breath parameters, while the whole-breath descriptors (R_{mean}, X_{mean} and AXV) did not differ (table 2). The Bland–Altman plots revealed small systematic biases for the 11 Hz estimates of ΔR, ΔX and AXV (online supplement figure S1 (available online at stacks.iop.org/PMEA/43/045004/mmedia)) and demonstrated that the widening of the agreement limits was due to the higher-impedance patients. Spearman correlation between the differences and the averages of the measures was significant only for X_{eI} ($P < 0.001$; data not shown) and AXV ($P = 0.01$). No significant difference was found between males and females in R_{mean} and X_{mean} at 10 and 11 Hz (table S2).

3.4. Explanatory simulations

The amplitude spectra of the $P(t)$ signal predicted by the model were computed with V'_{br} at different rates; for clarity, sinusoidal breathing was assumed (figure 5). Slow breathing resulted in densely spaced modulation side frequencies, whereas with increasing f_{br} the overlap of the 11 and 13 Hz side lobes widened, resulting stronger cross-talk and mutual bias in the Zrs values. Importantly, the modulation side lobes in P due to volume

Figure 4. Comparison of 10 and 11 Hz estimates of reactance (X10 and X11, respectively) at end expiration (a) and end inspiration (b), their differences (ΔX, (c)), the mean values for whole breathing cycles (d) and the reactance versus volume loop areas (AXV, (e)). Solid line: line of identity; dashed line: regression line; r^2: correlation coefficient.
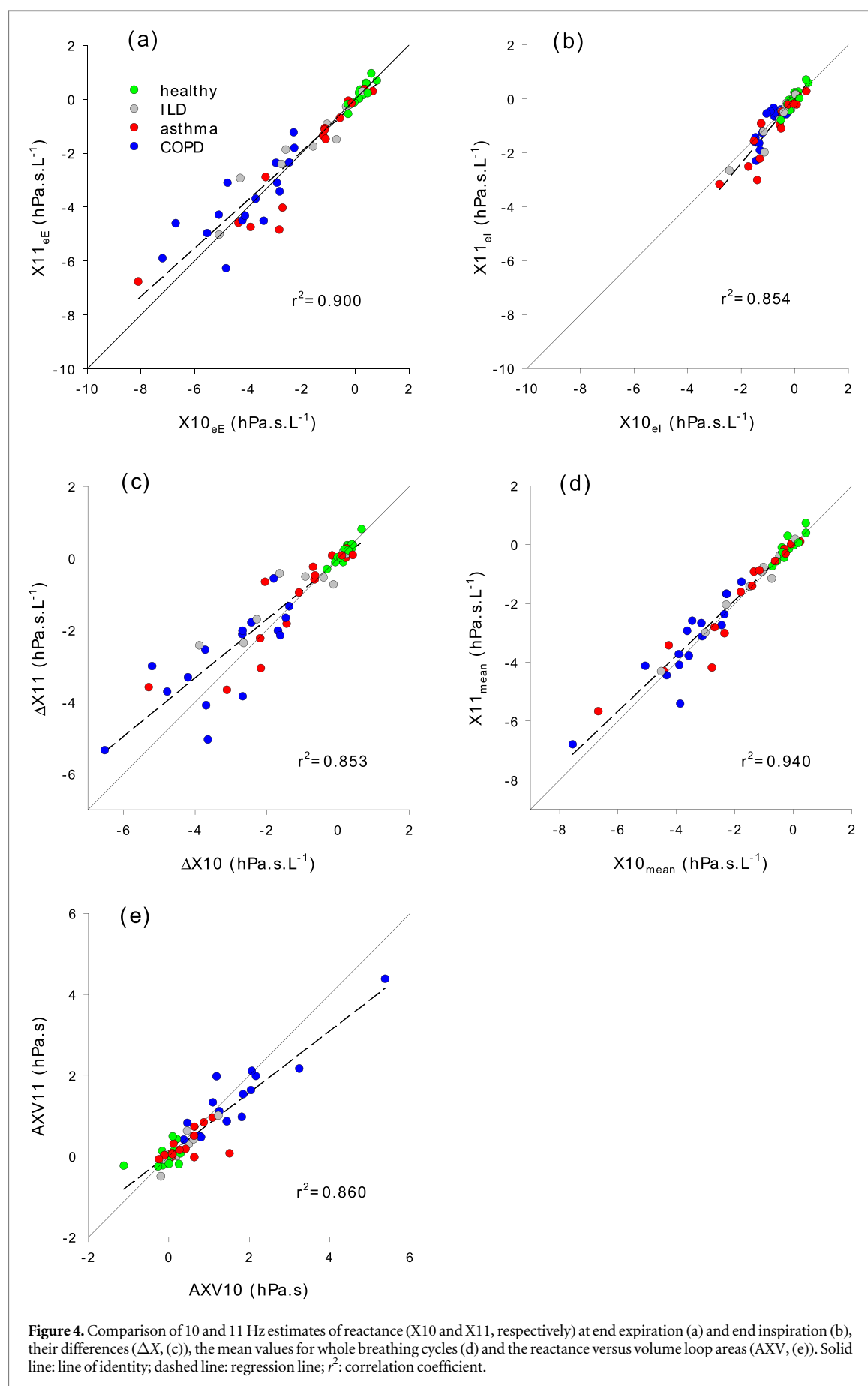
Table 1. Comparison of values of spirometry and intra-breath oscillometry measures obtained from single-frequency (10 Hz) measurements and those at 11 Hz extracted from multiple-frequency (5–37 Hz) oscillations.

	10 Hz median (25%; 75% IQR)		11 Hz median (25%, 75% IQR)		P
V_T (ml)	0.75	(0.54; 0.92)	0.78	(0.59; 0.95)	0.613
f_{br} (min^{-1})	15.2	(12.4; 19.9)	14.8	(12.4; 20.0)	0.940
R_{mean} (hPa.s.L^{-1})	3.60	(2.66; 4.90)	3.86	(2.60; 4.82)	0.841
R_{eE} (hPa.s.L^{-1})	3.72	(2.60; 4.92)	3.75	(2.72; 4.88)	0.745
R_{eI} (hPa.s.L^{-1})	2.70	(1.83; 3.57)	2.89	(2.07; 3.91)	0.200
ΔR (hPa.s.L^{-1})	0.77	(0.45; 1.55)	0.62	(0.30; 1.24)	0.213
$\Delta R/V_T$ (hPa.s.L^{-2})	1.20	(0.47; 1.88)	0.75	(0.32; 1.37)	0.103
X_{mean} (hPa.s.L^{-1})	−1.41	(−3.15; −0.31)	−1.27	(−3.01; −0.18)	0.758
X_{eE} (hPa.s.L^{-1})	−1.20	(−3.72; −0.03)	−1.48	(−4.02; −0.06)	0.983
X_{eI} (hPa.s.L^{-1})	−0.49	(−1.18; −0.09)	−0.47	(−1.22; −0.13)	0.790
ΔX (hPa.s.L^{-1})	−0.91	(−2.64; 0.15)	−0.57	(−2.23; 0.08)	0.898
$\Delta X/V_T$ (hPa.s.L^{-2})	−1.50	(−3.86; 0.14)	−0.91	(−3.30; 0.11)	0.983
AXV (hPa.s)	0.29	(0.03; 1.09)	0.18	(0.00; 0.84)	0.540

(IQR: interquartile range; P: level of statistical significance for the difference between median values at 10–11 Hz; V_T: tidal volume; f_{br}: breathing rate; R_{mean} and X_{mean}, R_{eE} and X_{eE}, R_{eI} and X_{eI}, ΔR and ΔX, respectively, stand for mean, end-expiratory, end-inspiratory values and their differences; AXV: area of the reactance-volume loop).

Table 2. Comparison of standard deviations of intra-breath oscillometry measures obtained from single-frequency (10 Hz) measurements and those at 11 Hz extracted from multiple-frequency (5–37 Hz) oscillations.

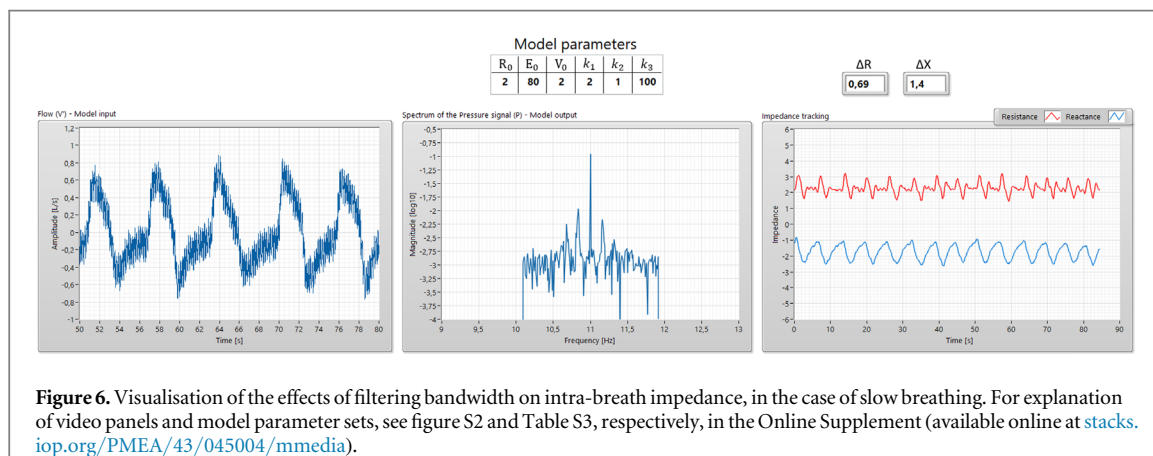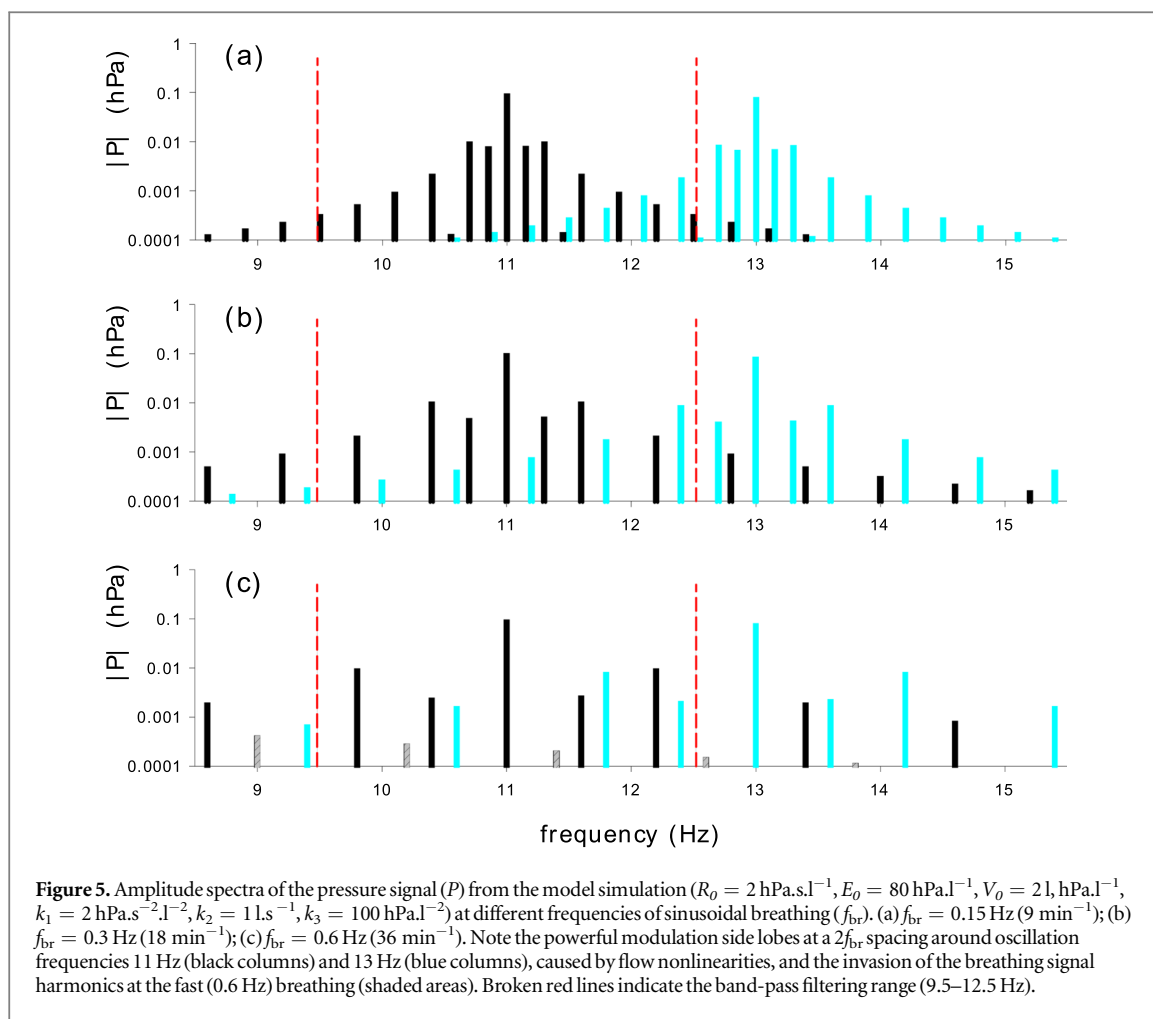|	10 Hz median (25%; 75% IQR)		11 Hz median (25%, 75% IQR)		P
R_{mean} (hPa.s.l^{-1})	0.27	(0.15; 0.39)	0.32	(0.20; 0.47)	0.080
R_{eE} (hPa.s.l^{-1})	0.33	(0.20; 0.64)	0.62	(0.32; 1.02)	**<0.001**
R_{eI} (hPa.s.l^{-1})	0.28	(0.18; 0.40)	0.42	(0.33; 0.60)	**<0.001**
ΔR (hPa.s.l^{-1})	0.41	(0.24; 0.65)	0.75	(0.47; 1.06)	**<0.001**
$\Delta R/V_T$ (hPa.s.l^{-2})	0.56	(0.32; 1.05)	0.99	(0.50; 1.63)	**0.003**
X_{mean} (hPa.s.l^{-1})	0.19	(0.10; 0.37)	0.26	(0.12; 0.46)	0.185
X_{eE} (hPa.s.l^{-1})	0.34	(0.13; 0.61)	0.52	(0.23; 0.91)	**0.018**
X_{eI} (hPa.s.l^{-1})	0.19	(0.12; 0.34)	0.30	(0.18; 0.52)	**<0.001**
ΔX (hPa.s.l^{-1})	0.36	(0.17; 0.63)	0.61	(0.31; 1.01)	**<0.001**
$\Delta X/V_T$ (hPa.s.l^{-2})	0.56	(0.23; 1.05)	0.78	(0.36; 1.77)	**0.020**
AXV (hPa.s)	0.24	(0.14; 0.36)	0.30	(0.18; 0.52)	0.067

(For abbreviations, see legend to table 1).

dependent nonlinearities in R and E (governed by coefficients k_2 and k_3, respectively), i.e. spaced at f_{br} and its multiples diminished fast. In contrast, the biphasic changes in R with V' (coefficient k_1) introduced strong side frequencies spaced at $2f_{br}$ and multiples, as expected from the rich harmonic content of a rectified V' signal.

Narrow band-pass ranges help keep away the interference from adjacent oscillatory components, although this may be achieved at the expense of modulation information. To illustrate this, intra-breath changes in R and X are visualised in the course of widening the band-pass range $\pm \Delta f$ around the 11 Hz oscillation frequency, by using V' signals recorded in a slowly-breathing (mean f_{br}=10.1 min^{-1}) and a fast breathing (29.6 min^{-1}) subject. Both simulations included the same 3 successive sets of model parameters (a–c) specified in the online supplement (table S3); the panels in the video files ((figures 6 and 7) are explained in the online supplement (figure S2). A narrow bandwidth $f_{br} < \Delta f < 2f_{br}$ enabled only the volume dependent modulations in R and X, while gradual inclusion of $2f_{br}$ and its multiples introduced the biphasic V' modulation in finer details—until the involvement of the modulation frequencies belonging to the 13 Hz oscillation impaired the quality of the intra-breath changes.

3.5. Breathing rate versus tracking frequency
In 5 selected subjects whose f_{br} ranged from the lowest (11.4 min^{-1}) to the largest value (29.6 min^{-1}), intra-breath changes were calculated while increasing the Δf bandwidth around 10 Hz from ± 0.25 to ± 3 Hz. Figure 8 illustrates ΔR and ΔX as functions of $\Delta f/f_{br}$, i.e. the number of modulation components included in the band-pass range. In agreement with the simulation results (see above), no intra-breath changes can be detected at $\Delta f/f_{br} < 1$. Even if natural fluctuations in f_{br} and asymmetrical breathing patterns are expected, the tidal changes in Zrs plateaued by 2–3 $\Delta f/f_{br}$ and can thus be recovered safely.

Figure 5. Amplitude spectra of the pressure signal (P) from the model simulation ($R_0 = 2\ \text{hPa.s.l}^{-1}$, $E_0 = 80\ \text{hPa.l}^{-1}$, $V_0 = 2\ \text{l, hPa.l}^{-1}$, $k_1 = 2\ \text{hPa.s}^{-2}.\text{l}^{-2}$, $k_2 = 1\ \text{l.s}^{-1}$, $k_3 = 100\ \text{hPa.l}^{-2}$) at different frequencies of sinusoidal breathing (f_{br}). (a) $f_{\text{br}} = 0.15\ \text{Hz}\ (9\ \text{min}^{-1})$; (b) $f_{\text{br}} = 0.3\ \text{Hz}\ (18\ \text{min}^{-1})$; (c) $f_{\text{br}} = 0.6\ \text{Hz}\ (36\ \text{min}^{-1})$. Note the powerful modulation side lobes at a $2f_{\text{br}}$ spacing around oscillation frequencies 11 Hz (black columns) and 13 Hz (blue columns), caused by flow nonlinearities, and the invasion of the breathing signal harmonics at the fast (0.6 Hz) breathing (shaded areas). Broken red lines indicate the band-pass filtering range (9.5–12.5 Hz).
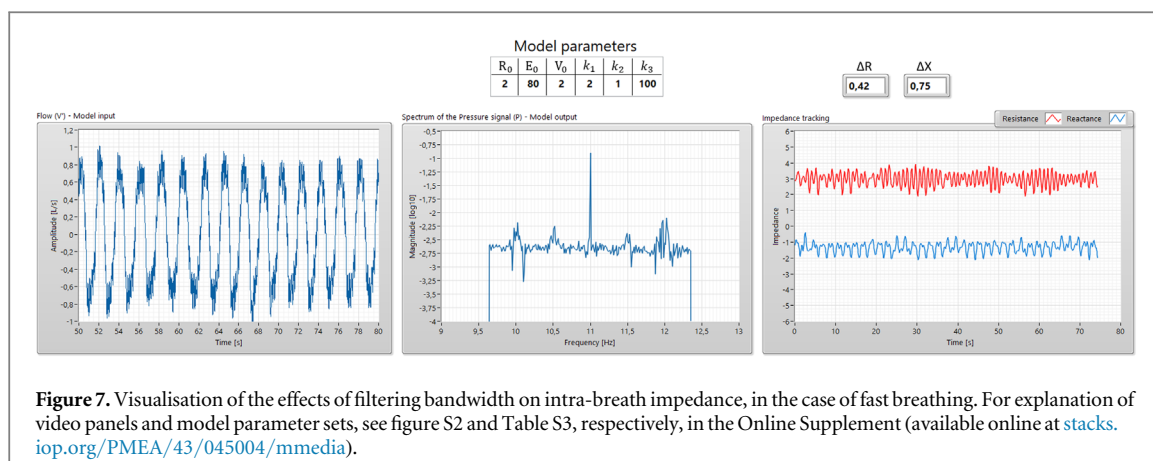

Figure 6. Visualisation of the effects of filtering bandwidth on intra-breath impedance, in the case of slow breathing. For explanation of video panels and model parameter sets, see figure S2 and Table S3, respectively, in the Online Supplement (available online at stacks. iop.org/PMEA/43/045004/mmedia).

4. Discussion

The main finding of the current study is a fairly good agreement between the corresponding mean values of the intra-breath measures at 10 and 11 Hz, although this is associated with less regular and uniform Zrs versus V loops and higher variability of data at 11 Hz. This good agreement also holds for the whole-breath mean values, which are the most closely related and reflect the within-session variability of measurements (figure 3(d)). The lack of statistically significant difference is somewhat surprising in the case of Xrs measures as one expects a monotonous increase in Xrs between 10 and 11 Hz, invariably in health and disease. In contrast, the changes in Rrs can be nonuniform: in healthy subjects, Rrs is expected to plateau at around 10 Hz (i.e., R10 ≈ R11) (Bates *et al* 2011, Oostveen *et al* 2013, Oostveen *et al* 2003), whereas in bronchial obstruction, such as in asthma and

Figure 7. Visualisation of the effects of filtering bandwidth on intra-breath impedance, in the case of fast breathing. For explanation of video panels and model parameter sets, see figure S2 and Table S3, respectively, in the Online Supplement (available online at stacks. iop.org/PMEA/43/045004/mmedia).
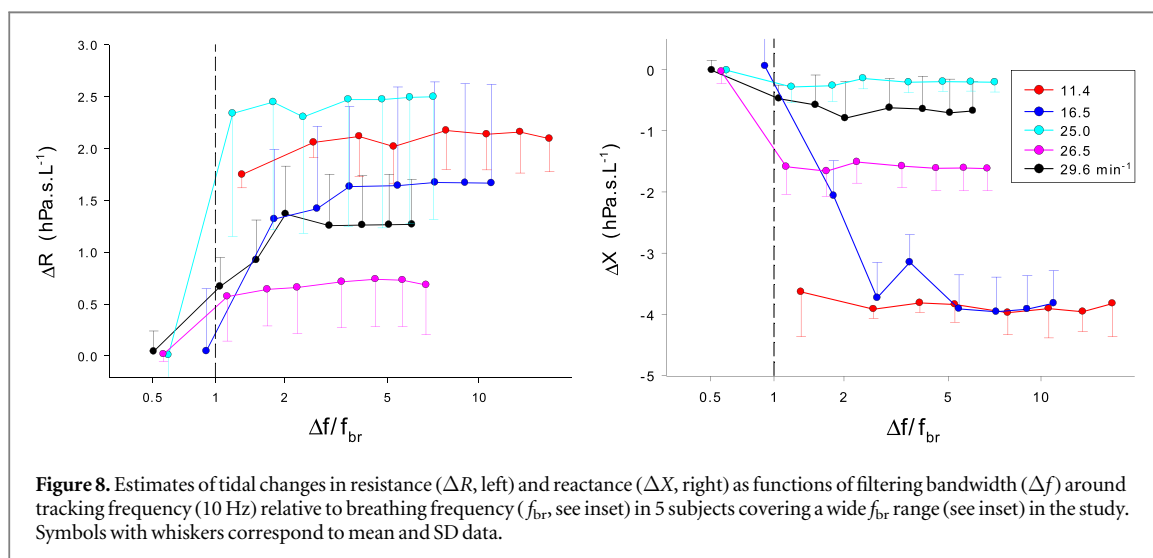
Figure 8. Estimates of tidal changes in resistance (ΔR, left) and reactance (ΔX, right) as functions of filtering bandwidth (Δf) around tracking frequency (10 Hz) relative to breathing frequency (f_{br}, see inset) in 5 subjects covering a wide f_{br} range (see inset) in the study. Symbols with whiskers correspond to mean and SD data.

COPD, the higher Rrs values are associated with a negative frequency dependence (R10 > R11) (Bates *et al* 2011, Goldman 2001, Oostveen *et al* 2003). Nevertheless, an increase in the population size may establish the significance of small differences due to frequency dependence of Zrs.

The primary reason for selecting 10 Hz for the sinusoidal oscillations was an ongoing multicenter study on intra-breath oscillometry that use this frequency in preschool-age children. The study has been conducted in the frame of a Clinical Research Collaboration Award from the European Respiratory Society (Sly and Hantos, 2018), which has resulted in measurements in >2000 children at 12 sites around the world since 2014. Additionally, the 0.1 s temporal resolution in Zrs made available in the research modality of tremoflo C-100 represents improvement to previous studies using 5 Hz (Dellacà *et al* 2004) or 8 Hz (Lorx *et al* 2017), and offers comparison to a close frequency (11 Hz) present in the widely employed composite oscillation signal.

Rrs was consistently lower at end inspiration than at end expiration ($\Delta R_{10} > 0$; see figure 3(c)), which can be attributed to the dilatation of the airways at a higher lung volume. The tidal change in Xrs was opposite in healthy subjects in whom inspiratory muscle tone (a stiffer chest wall) results in a slight decrease in Xrs ($\Delta X > 0$), compared to patients with lung disease in whom the increase in Xrs reflects the improving homogeneity of the lungs with increasing V ($\Delta X < 0$; see also figures 4(a) and (b)). Notwithstanding the physiological importance of the tidal changes in Rrs and Xrs, our data also indicate higher degrees of intra-breath fluctuations with V' than with V.

The possible mechanisms underlying the poorer loop shapes and the higher intraindividual variability of the intra-breath measures at 11 Hz are (i) the smaller amplitude of this oscillatory component resulting in a lower signal-to-noise level, (ii) the modulation of V' and, to a lesser extent, V with the 1 Hz fundamental frequency oscillations which may blur the zero-flow readings of R and X, and (iii) the corrupting effect of the adjacent 13 Hz signal component. This latter factor was clearly identified by the simulation study and is considered the most influential. It is obvious that the larger the intra-breath changes in Zrs the more powerful spectral side lobes conveying the amplitude modulation information develop around the oscillation frequencies. Additionally, with increasing f_{br} these side lobes move farther from their carrier frequency (e.g. 13 Hz) and invade more into

the side lobe region of the nearby (i.e. 11 Hz) component (see figure 5). It is also important to recall that the flow nonlinearities increase Rrs in both inspiration and expiration (Davidson *et al* 1986b, Horowitz *et al* 1983, Peslin *et al* 1971, Davidson *et al* 1986a), thereby introducing modulation side lobes at $2f_{br}$ and its multiples around each oscillation frequency. Narrow band-pass ranges would decrease the cross-talk between oscillation frequencies but this may result in a loss of information on the intra-breath modulation. Fast breathing is also associated with more rapid changes in Zrs within the time window of the calculation of spectra, which would bias the values at fast transitions, i.e. zero-flow, in particular; this has been pointed out in another simulation study (Alamdari *et al* 2019b). Unfortunately, these factors are enhanced in the case of paediatric patients who in turn are a privileged target population because of the low cooperation demand of oscillometry (Beydon *et al* 2007, Czövek *et al* 2016).

The problem addressed above would be eliminated largely if one of the closely spaced relative prime signal component pairs is omitted from the oscillation spectrum; it is otherwise questionable whether or not the presence of these adjacent frequencies (e.g. 11–13, 17–19 and 29–31 Hz) has any benefit in the quality of the Zrs spectra. According to the current specifications of one of oscillometry devices that use relative prime frequencies (RESTECH, 2022) these pairs of frequencies are no longer included in the oscillation signal. Further studies are needed to ascertain whether carefully designed 'pruned' frequency spectra ensure good intra-breath quality at selected frequencies. Additionally, many breathing cycles collected from long and multiple recordings may help reduce the variability and increase the robustness of the tracking estimates.

Finally, a potential study limitation is the small subject number precluding a reasonable analysis of the possible influence of sex on our results. Similar to other pulmonary function tests, oscillometry prediction equations are sex specific (Oostveen *et al* 2013) and desegregation of results by sex is desirable. The present study design controls for any such bias by using each subject as his or her own control when comparing 10 and 11 Hz results. Another limitation of this study is the absence of the paediatric age range; therefore, the conclusions that faster breathing increases the cross-talk between oscillation frequencies and the bias in the derived intra-breath measures need to be confirmed in future work.

In summary, the present investigation on the possibility to extract useful intra-breath indices of respiratory mechanics from conventional multiple-frequency oscillometry concludes with a positive message. On the basis of data from a small mixed population from an adult pulmonology practice it appears that the 'proxy' intra-breath measures at 11 Hz yield average values (although with a higher variance) close to those obtained specifically from tracking measurements at 10 Hz. Re-analysis of conventional oscillometry measurements is thus possible, and it may add dynamic, intra-breath measures to better characterise the status of respiratory mechanics.

Acknowledgments

Author contributions

GM, RJD, ZG and ZH designed the study; RJD organised the oscillometry data; GM and ZH analysed the intra-breath recordings; GM, ZG and ZH designed the simulation study; GM, RJD and ZH drafted the manuscript; all authors contributed to the article and approved the submitted version.

Conflicting interests

RJD acknowledges unrestricted educational grants from AstraZeneca, Boehringer-Ingelheim, Novartis, Pfizer and Teva Pharma which were applied to various parts of this project. GM, ZG and ZH has nothing to declare.

Ethics

The study had local IRB approval (McGill University Health Centre Authorization to Conduct Human Subjects Research, 14-467-BMB, and Comité d'éthique de CIUSSS de l'Ouest-de-l'île-de-Montréal Ethics Committee, SMHC #17–34). All participants gave informed consent to the investigation.

ORCID iDs

Gergely Makan ⓘ https://orcid.org/0000-0001-6648-6371
Ronald J Dandurand ⓘ https://orcid.org/0000-0003-3235-7824
Zoltán Gingl ⓘ https://orcid.org/0000-0001-6570-2685
Zoltán Hantos ⓘ https://orcid.org/0000-0002-5696-7750

References

Alamdari H H, El-Sankary K and Maksym G N 2019a Time-varying respiratory mechanics as a novel mechanism behind frequency dependence of impedance: a modeling approach *IEEE Trans. Biomed. Eng.* **66** 2433–46

Alamdari H H, El-Sankary K, Peters U, Amer A L, Milne M, Henzler A, D Brown J A and Maksym G N 2019b Tracking respiratory mechanics with oscillometry: introduction of time-varying error *IEEE Sens. J.* **19** 311–21

Bates J H T, Irvin C G, Farré R and Hantos Z 2011 Oscillation mechanics of the respiratory system *Compr Physiol.* **1** 1233–72

Beydon N *et al* 2007 An official american thoracic society/european respiratory society statement: pulmonary function testing in preschool children *Am. J. Respir Crit Care Med.* **175** 1304–45

Bland J M and Altman D G 1986 Statistical methods for assessing agreement between two methods of clinical measurement *Lancet* **1** 307–10

Chiabai J, Friedrich F O, Fernandes M T C, Serpa F S, Antunes M O B, Neto F B, Makan G, Hantos Z, Sly P D and Jones M H 2021 Intrabreath oscillometry is a sensitive test for assessing disease control in adults with severe asthma *Ann. Allergy Asthma Immunol.* **127** 372–7

Czövek D *et al* 2016 Tidal changes in respiratory resistance are sensitive indicators of airway obstruction in children *Thorax* **71** 907–15

Daroczy B and Hantos Z 1990 Generation of optimum pseudorandom signals for respiratory impedance measurements *Int. J. Biomed. Comput.* **25** 21–31

Davidson R N, Greig C A, Hussain A and Saunders K B 1986a Within-breath changes of airway caliber in patients with air-flow obstruction by continuous measurement of respiratory impedance *Br. J. Dis. Chest* **80** 335–52

Davidson R N, Hayward L, Pounsford J C and Saunders K B 1986b Lung function and within-breath changes in resistance in patients who have had a laryngectomy *Q. J. Med.* **60** 753–62

Dellacà R L, Santus P, Aliverti A, Stevenson N, Centanni S, Macklem P T, Pedotti A and Calverley P M A 2004 Detection of expiratory flow limitation in COPD using the forced oscillation technique *Eur. Respir J.* **23** 232–40

Goldman M D 2001 Clinical application of forced oscillation *Pulm Pharm Ther.* **14** 341–50

Gray D M *et al* 2018 Intra-breath measures of respiratory mechanics in healthy African infants detect risk of respiratory illness in early life *Eur. Respir J.* **53** 1800998

Hantos Z 2021 Intra-breath oscillometry for assessing respiratory outcomes *Curr. Opin. Physiol.* **22** 100441

Horowitz J G, Siegel S D, Primiano F P Jr and Chester E H 1983 Computation of respiratory impedance from forced sinusoidal oscillations during breathing *Comput. Biomed. Res.* **16** 499–521

Kaczka D W and Dellaca R L 2011 Oscillation mechanics of the respiratory system: applications to lung disease *Crit. Rev. Biomed. Eng.* **39** 337–59

Kalchiem-Dekel O and Hines S E 2018 Forty years of reference values for respiratory system impedance in adults: 1977-2017 *Respir Med.* **136** 37–47

Làndsér F J, Nagels J, Demedts M, Billiet L and Van De Woestijne K P 1976 A new method to determine frequency characteristics of the respiratory system *J. Appl. Physiol.* **41** 101–6

Lorx A *et al* 2017 Airway dynamics in COPD patients by within-breath impedance tracking: effects of continuous positive airway pressure *Eur. Respir J.* **49** 1601270

Michaelson E D, Grassman E D and Peters W R 1975 Pulmonary mechanics by spectral analysis of forced random noise *J. Clin. Invest.* **56** 1210–30

Nagels J, Làndsér F J, Van Der Linden L, Clément J and Van De Woestijne K P 1980 Mechanical properties of lungs and chest wall during spontaneous breathing *J. Appl. Physiol.* **49** 408–16

Oostveen E, Boda K, Der Grinten V, James C P M, Young A L, S, Nieland H and Hantos Z 2013 Respiratory impedance in healthy subjects: baseline values and bronchodilator response *Eur. Respir J.* **42** 1513–23

Oostveen E, Macleod D, Lorino H, Farre R, Hantos Z, Desager K and Marchal F 2003 The forced oscillation technique in clinical practice: methodology, recommendations and future developments *Eur. Respir J.* **22** 1026–41

Peslin R, Hixon T and Mead J 1971 Variations des résistances thoraco-pulmonaires au cours du cycle ventilatoire étudiees par méthode d'oscillation [Variations of thoraco-pulmonary resistance during the respiratory cycle studied by the oscillation method] *Bull Physio-path Respir (Nancy)* **7** 173–88

Peslin R, Ying Y, Gallina C and Duvivier C 1992 Within-breath variations of forced oscillation resistance in healthy-subjects *Eur. Respir J.* **5** 86–92 (PMID: 1577156)

RESTECH 2022 *Resmon Pro Full (V3)* [Online]. Available https://restech.it/project/resmon-pro-full/ (Accessed: 4 January 2022)

Rohrer F 1915 Der Strömungswiderstand in den menschlichen Atemwegen und der Einfluss der unregelmässigen Verzweigung des Bronchialsystems auf den Atmungsverlauf in verschiedenen Lungenbezirken *Pflügers Arch Ges Physiol.* **162** 225–99

Sly P D and Hantos Z 2018 The international collaboration to improve respiratory health in children (INCIRCLE) *Eur. Respir J.* **52** 1801867